



different types of double bonds, the reaction proceeds with high regioselectivity and sometimes removal of CO occurs (Scheme 1). However, the mechanisms of these reactions are not well understood.

Inspired by the intriguing results,<sup>8</sup> we performed theoretical calculations to investigate the detailed reaction mechanisms of the cycloaddition chemistry of  $\text{PCO}^-$  (Scheme 1), including the reactivity and selectivity of substrates with different unsaturated bonds. Our findings may open a new avenue for further development of  $\text{PCO}^-$  chemistry.

On the basis of the experimental results, the cycloadditions of  $\text{PCO}^-$  with different unsaturated compounds proceed with high regioselectivity. For example,  $\text{Na}(\text{PCO})$  was treated with 2.0 equiv. of an asymmetrical alkyne ( $\text{EtO}_2\text{CC}\equiv\text{CPh}$ ) to form **1** as the only product (Scheme 1, right).<sup>8b</sup> More importantly, the more electron-deficient alkyne ( $\text{EtO}_2\text{CC}\equiv\text{CCO}_2\text{Et}$ ) did not generate only **2**, but also **2'** with the loss of CO (Scheme 1, left).<sup>8b</sup> Significant uncertainties exist concerning the observed chemical selectivities, in particular on the high regioselectivity and the process of removal of CO from the formed heterocycle. Thus, we first investigated the cycloadditions of  $\text{PCO}^-$  and alkynes through DFT calculations at the M06-2X/6-311++G(2d,p)//B3LYP-D/6-31+G(d) level (see the ESI† for details).

The proposed reaction pathway for the first [2+2] cycloaddition of  $\text{EtO}_2\text{CC}\equiv\text{CPh}$  and  $\text{PCO}^-$ , including the computed free energies is shown in Fig. 2. All efforts made towards locating a transition state for a concerted [2+2] cycloaddition reaction failed. Instead, a nucleophilic attack of the phosphorus atom in  $\text{PCO}^-$  on C1 and C2 of the alkyne could be identified. Interestingly, the nucleophilic attack on C1 (**TS1A'**, 27.1 kcal mol<sup>-1</sup>) is significantly higher than that on C2 (**TS1A**, 19.4 kcal mol<sup>-1</sup>), which could be mainly attributed to the electronic effects (Fig. 3). For instance, natural population analysis (NPA) indicates that the charges of C1 and C2 in  $\text{EtO}_2\text{CC}\equiv\text{CPh}$  are  $-0.10$  and  $0.07e$ , respectively, whereas that of P in  $\text{PCO}^-$  is  $-0.44e$ , indicating that  $\text{PCO}^-$  is more favoured to attack C2. This is in line with the experimental observations that only **1** was formed (Scheme 1).<sup>8b</sup> It is important to note that the charge of oxygen in  $\text{PCO}^-$  is  $-0.70e$ , indicating that the oxygen might attack C2. However, no stable intermediate of C2-O bond formation could be identified.<sup>10</sup> Indeed, the HOMO of  $\text{PCO}^-$  is mainly localized at the  $\pi$  orbital of the P centre. The absolute maximum of the coefficient at P (0.51) is much larger than that at O (0.30). Therefore, attacking alkynes *via* the P centre could lead to favorable orbital overlap between the  $\text{PCO}^-$   $\pi$  orbital and the alkyne  $\pi^*$  orbitals (LUMOs).

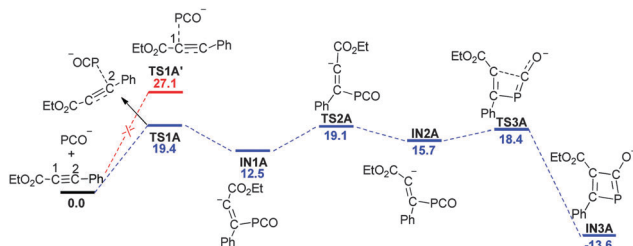


Fig. 2 Free energy profile for the first [2+2] cycloaddition of  $\text{EtO}_2\text{CC}\equiv\text{CPh}$  and  $\text{PCO}^-$ . The values are given in kcal mol<sup>-1</sup>.

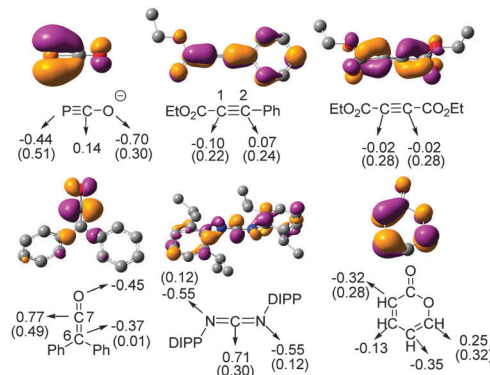


Fig. 3 HOMO of  $\text{PCO}^-$  and LUMOs of unsaturated compounds (isovalue = 0.05). NPA partial charges are given in  $e$ . Absolute maxima of the coefficients at the reacting termini are given in parentheses.

Subsequently, **IN1A** is formed with the  $\text{CO}_2\text{Et}$  group on the same side of  $\text{PCO}$ , which is sterically unfavourable for the next C-C bond formation. Thus, an isomerization step was located with an activation energy of 6.6 kcal mol<sup>-1</sup>. From **IN2A** (15.7 kcal mol<sup>-1</sup>), a four-membered transition state **TS3A** (18.4 kcal mol<sup>-1</sup>) occurred, leading to the first [2+2] cycloaddition product **IN3A** ( $-13.6$  kcal mol<sup>-1</sup>).

Fig. 4 depicts the second [2+2] cycloaddition of  $\text{EtO}_2\text{CC}\equiv\text{CPh}$  and  $\text{PCO}^-$ . In a similar way, very stable **1** ( $-88.9$  kcal mol<sup>-1</sup>) is generated *via* nucleophilic attack of the P atom, isomerization and C-C bond formation. It is important to note that the final process is highly exergonic (**TS6A**  $\rightarrow$  **1**). According to the computed NICS(1)<sub>zz</sub><sup>11</sup> value of **1** ( $-13.4$  ppm), the significant stability is mainly attributed to the release of ring strain and the gain of aromaticity in **1**.

We next turned our attention to the loss of CO, which is observed by using the more electron-deficient alkyne ( $\text{EtO}_2\text{CC}\equiv\text{CCO}_2\text{Et}$ ) as the substrate (Scheme 1, left). Similar to **1**, a six-membered aromatic product **2** is formed ( $-100.5$  kcal mol<sup>-1</sup>) (see the ESI† for details). Direct removal of CO from **2** is found to be too energy demanding to take place (Fig. 5, right). Alternatively, from **IN5B**, a formal [3+2] cycloaddition with the loss of CO could be located *via* two steps (Fig. 5, left). The activation barriers for the transformation are only 2.2 and 0.3 kcal mol<sup>-1</sup>. The free energies of **TS5B** and **TS7B** are  $-34.0$  and  $-35.2$  kcal mol<sup>-1</sup>, which are 3.4 and 2.2 kcal mol<sup>-1</sup> higher than that of **IN5B**, respectively, indicating that both processes could readily occur, in agreement with the experimental observations that **2** and **2'** were generated. In addition, when  $\text{EtO}_2\text{CC}\equiv\text{CPh}$  was used as the substrate (Fig. 4), the activation energy of C3 attacking C5

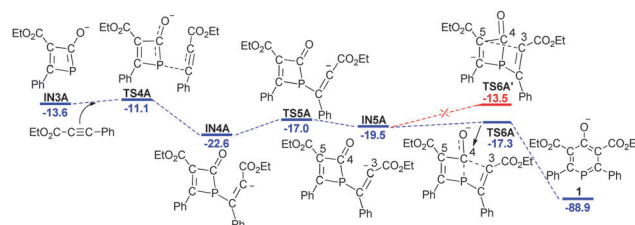


Fig. 4 Free energy profile for the second [2+2] cycloaddition of  $\text{EtO}_2\text{CC}\equiv\text{CPh}$  and  $\text{PCO}^-$ . The values are given in kcal mol<sup>-1</sup>.



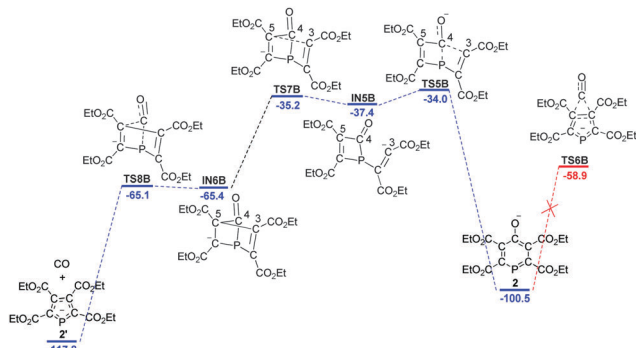


Fig. 5 Free energy profile for the CO removal process using  $\text{EtO}_2\text{CC}\equiv\text{CCO}_2\text{Et}$  and  $\text{PCO}^-$  as substrates. The values are given in  $\text{kcal mol}^{-1}$ .

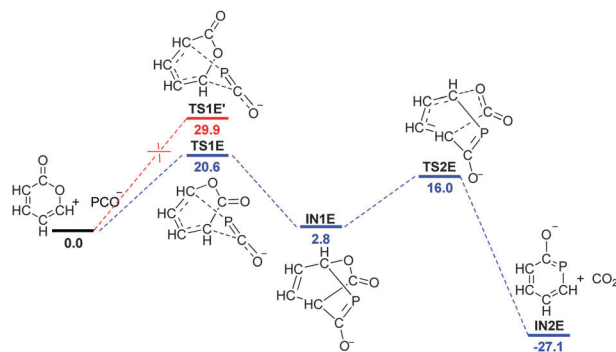


Fig. 6 Free energy profile for the [4+2] cycloaddition using  $2H$ -pyran-2-one and  $\text{PCO}^-$  as substrates. The values are given in  $\text{kcal mol}^{-1}$ .

is  $6.0 \text{ kcal mol}^{-1}$  ( $\text{TS6A}'$ ), which is approximately 2 times higher than that of C3 attacking C4 ( $\text{TS6A}$ ,  $2.2 \text{ kcal mol}^{-1}$ ), explaining why **1** was formed exclusively during the reaction.

To gain more insight into the cycloaddition chemistry of  $\text{PCO}^-$ , the regioselectivities<sup>8a</sup> of its outcome with  $\text{Ph}_2\text{C}=\text{C}=\text{O}$  and  $\text{DIPPN}=\text{C}=\text{NDIPP}$  were also studied (see the ESI† for details). The results showed that these two transformations do not proceed in a concerted fashion, but are stepwise and initiated by a nucleophilic attack of the phosphorus centre of  $\text{PCO}^-$ , which is similar to what was discussed above. The regioselectivities were determined by the nature of electronic properties of substrates as illustrated in Fig. 3. For example, it is much easier for  $\text{PCO}^-$  to attack C7 ( $0.77e$ ) over C6 ( $-0.37e$ ). The activation energy is  $4.6 \text{ kcal mol}^{-1}$ , which is significantly lower than that of attacking C6 ( $37.0 \text{ kcal mol}^{-1}$ ).

Finally, we examined the [4+2] cycloaddition between  $2H$ -pyran-2-one and  $\text{PCO}^-$  (Fig. 6).<sup>8b</sup> According to the experimental study, a distinct gas evolution ( $\text{CO}_2$ ) is observed. Very interestingly, the transformation involves two concerted steps, including a Diels–Alder-type cycloaddition and a rearrangement involving

the removal of  $\text{CO}_2$ . The electronic effects also play a key role in this reaction. The favourable reactive sites lead to the lower barrier process ( $\text{TS1E}$ ,  $20.6 \text{ kcal mol}^{-1}$ ). Our calculations showed that the  $\text{NICS}(1)_{zz}$  value of **IN2E** is  $-15.2 \text{ ppm}$  and the entropy change of the rearrangement step is  $43.3 \text{ cal mol}^{-1} \text{ K}^{-1}$  (**IN1E**  $\rightarrow$  **IN2E**), indicating that the resulting aromaticity and entropy increase are the driving force for the transformation.

We have computationally characterized the mechanisms for the [2+2], [3+2] and [4+2] cycloaddition chemistry of  $\text{PCO}^-$  with different unsaturated compounds, including alkynes, ketenes, carbodiimides and  $2H$ -pyran-2-one. The results showed that the [2+2] and [3+2] cycloaddition of  $\text{PCO}^-$  favoured stepwise processes, whereas [4+2] cycloaddition is a concerted process. More importantly, electronic effects play a key role in the regioselectivities of cycloadditions. Our findings can serve as a clue for further development of  $\text{PCO}^-$  chemistry.

This work was supported by the National Basic Research Program of China (2012CB821600, 2013CB910700 and 2011CB808504), the Chinese National Natural Science Foundation (21232005, 21375113, and 21103142), the Program for New Century Excellent Talents in University (NCET-13-0511), and the Program for Changjiang Scholars and Innovative Research Team in University and the Fundamental Research Funds for the Central Universities (2012121021). Thanks are also given to the China Scholarship Council for a Graduate Fellowship (L.L.). L. L. thanks the D. A. Ruiz from UCSD for valuable discussion.

## Notes and references

- 1 T. E. Gier, *J. Am. Chem. Soc.*, 1961, **83**, 1769.
- 2 F. Mathey, *Angew. Chem., Int. Ed.*, 2003, **42**, 1578.
- 3 G. Becker, W. Schwarz, N. Seidler and M. Westerhausen, *Z. Anorg. Allg. Chem.*, 1992, **612**, 72.
- 4 S. Alidori, D. Heift, G. Santiso-Quinones, Z. Benkó, H. Grützmacher, M. Caporali, L. Gonsalvi, A. Rossin and M. Peruzzini, *Chem. – Eur. J.*, 2012, **18**, 14805.
- 5 D. Heift, Z. Benko and H. Grützmacher, *Dalton Trans.*, 2014, **43**, 5920.
- 6 A. M. Tondreau, Z. Benko, J. R. Harmer and H. Grützmacher, *Chem. Sci.*, 2014, **5**, 1545.
- 7 A. R. Jupp and J. M. Goicoechea, *J. Am. Chem. Soc.*, 2013, **135**, 19131.
- 8 (a) A. R. Jupp and J. M. Goicoechea, *Angew. Chem., Int. Ed.*, 2013, **52**, 10064; (b) X. Chen, S. Alidori, F. F. Puschmann, G. Santiso-Quinones, Z. Benkó, Z. Li, G. Becker, H.-F. Grützmacher and H. Grützmacher, *Angew. Chem., Int. Ed.*, 2014, **53**, 1641; (c) D. Heift, Z. Benkó and H. Grützmacher, *Angew. Chem., Int. Ed.*, 2014, **53**, 6757.
- 9 D. Heift, Z. Benko and H. Grützmacher, *Dalton Trans.*, 2014, **43**, 831.
- 10 All efforts failed to locate an intermediate of C2–O bond formation. The bond breaks up into  $\text{EtO}_2\text{CC}\equiv\text{CPh}$  and  $\text{PCO}^-$  immediately during the optimization process.
- 11 (a) P. v. R. Schleyer, C. Maerker, A. Dransfeld, H. Jiao and N. J. R. v. E. Hommes, *J. Am. Chem. Soc.*, 1996, **118**, 6317; (b) H. Fallah-Bagher-Shaidaei, C. S. Wannere, C. Corminboeuf, R. Puchta and P. v. R. Schleyer, *Org. Lett.*, 2006, **8**, 863; (c) J. Zhu, K. An and P. v. R. Schleyer, *Org. Lett.*, 2013, **15**, 2442; (d) K. An and J. Zhu, *Eur. J. Org. Chem.*, 2014, 2764.

